Pain reflects the informational value of nociceptive inputs.

Michel-Pierre Coll[1,2], Zoey Walden[3], Pierre-Alexandre Bourgoin[4], Véronique Taylor[5], Pierre Rainville[6,7], Manon Robert[8], Dang Khoa Nguyen[8], Pierre Jolicoeur[9] and Mathieu Roy*[3,10]

[1]École de Psychologie, Université Laval, Québec, QC, Canada.
[2]Centre interdisciplinaire de recherche en réadaptation et intégration sociale (CIRRIS), Québec, QC, Canada
[3]Department of Psychology, McGill University, 2001 McGill College, Montréal, QC, Canada.
[4]Department of Psychology, Université du Québec à Montréal, Montreal, QC, Canada
[5]Department of Epidemiology, Brown University, 121 South Main St, Providence, RI, 02903
[6]Research Center of the Institut Universitaire de Gériatrie de Montréal, Université de Montréal, Montréal, QC, Canada
[7]Department of Stomatology, Université de Montréal, Montréal, QC, Canada
[8]Centre de Recherche du Centre Hospitalier de l'Université de Montréal (CRCHUM), Université de Montréal, Montréal, QC, Canada
[9]Department of Psychology, Université de Montréal, Montréal, QC, Canada
[10]Alan Edwards Centre for Research on Pain, McGill University, Montreal, QC, Canada.
*Correspondance to: mathieu.roy3@mcgill.ca

Abstract

Pain perception and its modulation are fundamental to human learning and adaptive behavior. This study investigated the hypothesis that pain perception is tied to pain's learning function. Thirty-one participants performed a threat conditioning task where certain cues were associated with a possibility of receiving a painful electric shock. The cues that signaled potential pain or safety were regularly changed, requiring participants to continually establish new associations. Using computational models, we quantified participants' pain expectations and prediction errors throughout the task and assessed their relationship with pain perception and electrophysiological responses. Our findings revealed that subjective pain perception increases with prediction error, that is when pain was unexpected. Prediction errors were also related to physiological nociceptive responses, including the amplitude of the nociceptive flexion reflex and EEG markers of cortical nociceptive processing (N2-P2 and gamma-band ERS). Additionally, higher pain expectations were related to increased late event-related potential responses and alpha/beta decreases in amplitude during cue presentation. These results further strengthen the idea of a crucial link between pain and learning and suggest that understanding the influence of learning mechanisms in pain modulation could help us understand when and why pain perception is modulated in health and disease.

Keywords: pain | learning | value | nociception

Acknowledgements
VT, PR, PJ and MR designed the study; PAB, MR, NDK created the materials and acquired the data; MP, ZW and MR analysed and interpreted the data and wrote the manuscript. All authors revised and approved the manuscript.

MPC was supported by a fellowship from the Canadian Institutes of Health Research and a career award from the Fonds de Recherche Québec–Santé (FRQS) during this work. This work was supported by a Discovery Grants from the Natural Sciences and Engineering Research Council of Canada (NSERC) to PR (Grant RGPIN-2013-06799), PJ (Grant RGPIN-2017-06679) and MR (Grant RGPIN-2016-06682) and a Canada Research Chair (CRC) in Brain Imaging of Experimental and Chronic Pain to MR and CRC in Experimental Cognitive Neuroscience to PJ. DKN is supported by the Canada Research Chairs Program, the Canadian Institutes of Health Research and the NSERC. PAB was supported by a scholarship from the FRQS in partnership with Parkinson Canada.

Code and data availability
Due to ethical constraints, we cannot openly share the raw data. BIDS formatted raw data are available on request. The code and instructions for reproducing all analyses and figures is available at https://github.com/mpcoll/eeg_painlearning_2023.

Introduction

Pain captures our attention and commands us to attend to potential sources of injuries. One important advantage of perceiving pain is that it allows reacting in a flexible and adaptive manner. Moreover, the effects of pain on behavior are not limited to immediately perceived pain. Indeed, pain not only serves as a warning signal, but it also teaches us to identify and avoid future threats (Seymour, 2019). In this study, we examined the possibility that pain perception could be modulated by the central nervous system to optimize pain's learning function. More specifically, we hypothesized that nociceptive processing may be amplified when pain is surprising to facilitate predictive learning about pain.

Learning theories propose that learning is initiated when a discrepancy arises between anticipated predictions and actual outcomes, a phenomenon referred to as prediction error. (PE; Sutton & Barto, 2018). PEs can be classified as either "signed" to discern between outcomes that are superior or inferior to expectations, or "unsigned" to include both kinds of surprising events. Signed PEs are essential for learning the aversive value of cues predicting pain, and we therefore hypothesized that perceived pain and nociceptive responses will increase with the magnitude of negative PEs.

Recent brain imaging studies have observed signed PEs in ascending nociceptive pathways, such as the periaqueductal gray and anterior cingulate cortex (Herry & Johansen, 2014; Jepma et al., 2022; Roy et al., 2014). However, it remains unclear whether these PE signals are produced in these regions or generated earlier in the spinal cord (McNally et al., 2011). Indeed, the dorsal horn of the spinal cord receives descending projections from the forebrain, that can regulate the transmission of nociceptive signals from spinal projection neurons. It is, therefore, judiciously positioned to integrate ascending nociceptive signals with descending information related to expected pain probability. Spinally generated prediction error signals could then be carried to the various cerebral targets of nociceptive pathways such as the periaqueductal gray, parabrachial nucleus and amygdala, thalamus, somatosensory cortices, insula, and anterior cingulate cortex (Price, 2000). Indeed, expectations of both

decreased pain (hypoalgesia) and increased pain (hyperalgesia) have been shown to modulate spinal responses to nociception (Cormier et al., 2013; Goffaux et al., 2007), which aligns with the notion that pain-related learning processes may mobilize cerebrospinal pathways. However. the effective contribution of lower-order nociceptive responses to the changes in cortical processing has been debated (Martini et al., 2015) and the dynamics of these modulatory processes have received little attention in the context of learning.

In a previous study, we demonstrated that the spinally-mediated nociceptive flexion reflex (NFR) amplitude was associated with learning parameters during a threat conditioning procedure, but the nature of the experimental design made it difficult to examine PEs specifically (Taylor et al., 2017). Moreover, the amplitude of the NFR also depends on the excitability of spinal motoneurons in addition to that of spinal nociceptive neurons, making it difficult to interpret the modulation of NFR when taken in isolation (Henrich et al., 2022). To overcome these limitations, we designed a study in which the reinforcement contingencies changed rapidly and combined the recording of NFR amplitude with electroencephalography (EEG) to link NFR modulation with the influx of ascending nociceptive signals to the cortex.

The N2-P2 somatosensory-evoked potentials is thought to originate from midline generators linked to pain's affective-motivational dimension (Garcia-Larrea et al., 2003). The amplitude of the N2-P2 is correlated with subjective pain reports (Colloca et al., 2008), but it has also been shown to reflect non-pain-specific aspects of somatosensory processing (Iannetti et al., 2008; Mouraux & Iannetti, 2009). By contrast, fluctuations in gamma band activity have recently been suggested as a more specific indicator of pain (Hu & Iannetti, 2019; Linde et al., 2023) and can be used to complement the N2-P2 as a cortical index of pain processing. Both EEG responses have been previously related to pain expectations (Strube et al., 2021). However, there is still a need for evidence to connect these EEG markers of pain processing to aversive prediction errors (PEs) specifically.

Finally, to understand how PEs are generated, it is also important to consider the cerebral processes associated with the expected probability of pain before it occurs. Here, we focused on two indices of expected

pain: the late positive potential, which peaks around 400-600 ms after the pain-predictive cue, and a decrease of oscillatory power in the alpha and beta bands (Nickel et al., 2022; Pavlov & Kotchoubey, 2018), which appear to gradually increase with pain expectations.

Results

Thirty-one healthy adults took part in a threat conditioning task, in which visual cues featuring neutral faces were either paired or unpaired with the potential of receiving a painful electric shock. Following an initial habituation block in which no shocks were delivered, participants completed six blocks. In each block, one of four displayed faces was paired with a painful shock to the sural nerve in 50% of the trials (CS+), while the other faces were never associated with the shock (CS-). Two new faces were introduced in each proceeding block, one becoming the new CS+ face and the other remaining a CS- face. CS+ faces from one block consistently transitioned to a CS-extinction (CS-E) face in the subsequent block (Figure 1a). Each reinforced CS+ face presentation terminated with a painful shock and was followed by a 2-second fixation cross, after which participants had up to 10 seconds to record their pain rating (Figure 1b). Throughout this paper, new CS- faces in each block are designated as CS-1, while CS- faces that were presented in a previous block are referred to as

CS-2. A face was not presented again after appearing in two blocks.

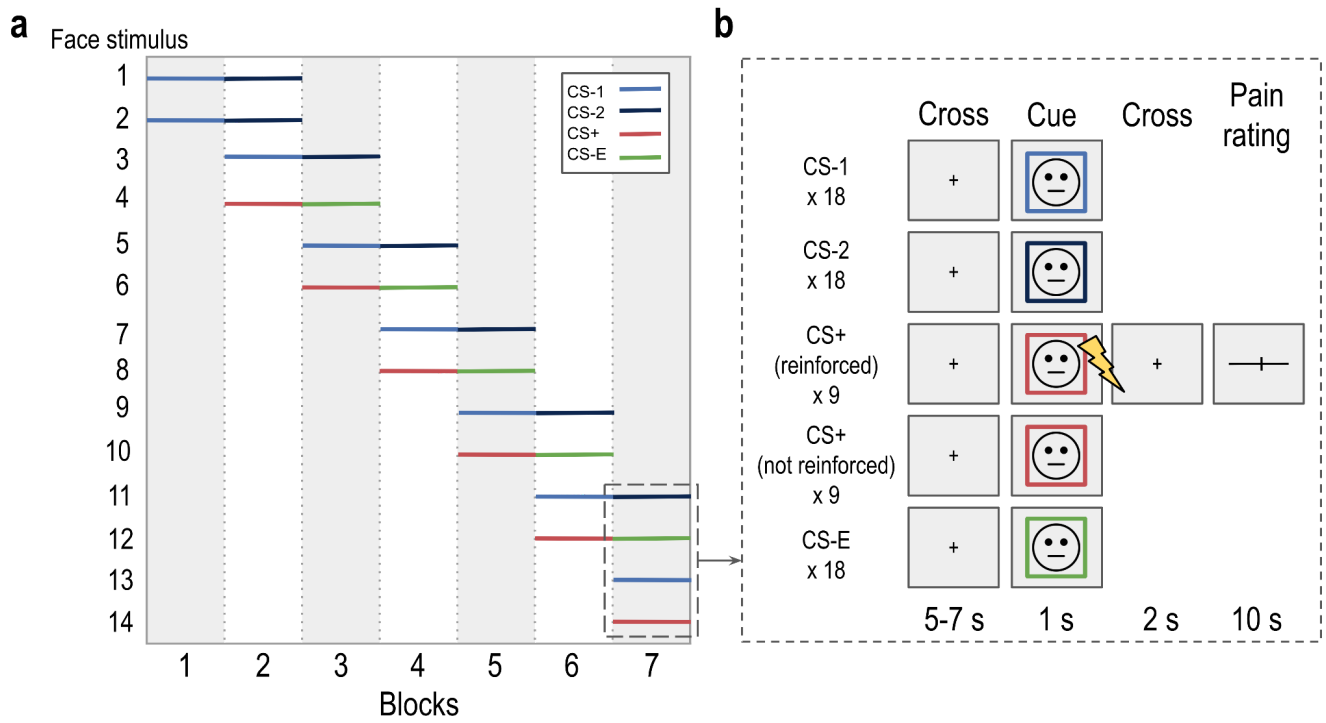

Figure 1. Illustration of the structure of the threat conditioning task. (a) The experiment began with the random presentation of two faces unpaired with electric shocks. After 18 presentations of each face, two new faces were introduced, one paired with shocks on 50% of trials (CS+), and one unpaired (CS-1), while the two initial faces were presented an additional 18 times (CS-2). Then, as the two initial faces stopped being presented, two new faces were introduced, one paired with shocks, and one unpaired, and the previously paired face became unpaired (CS-E). Each face was presented a total of 36 times, except for the last two faces, each presented 18 times. **(b) Illustration of the trial structure within blocks 2 to 7**. For each trial, a fixation cross was first presented for 5 to 7 s, followed by the CS for 1 s. Different colors indicate different CS identities. Shocks were delivered at the offset of 50% of the CS+, followed by a fixation cross (2s) and a visual analog scale (VAS) displayed for pain ratings (10s).

Skin conductance responses and computational modeling

Skin conductance response (SCR) amplitude at each trial served as an indicator of novelty and learned shock expectations (Figure 2a), displaying higher responses for new stimuli (CS-1) and stimuli previously associated with a shock (CS+). A linear mixed model verified that SCR varied among the four stimulus conditions (CS-1, CS-2, CS+, CS-E) [$\chi^2(3) = 249.31$, $p < 0.001$]. This effect interacted with block number [$\chi^2(1) = 29.51$, p

< 0.001], indicating that the SCR response to CS+ was higher in block 1 than in other blocks [$\chi^2(1) = 15.20$, $p < 0.001$], while the other conditions did not vary across blocks [ps > 0.07].

To quantify participants' learning dynamics throughout the task, we evaluated the ability of various computational learning models to account for variations in single-trial SCR. Specifically, we compared the Rescorla-Wagner model (Rescorla & Wagner, 1972), a Pearce-Hall hybrid model (RW/PH, Pearce & Hall, 1980), and a two-level Hierarchical Gaussian Filter (HGF-2) model (Mathys et al., 2014). Each had two different versions; the first version allowed updating expectations for all previously seen cues when one cue was reinforced (inter-cue), and another version allowed updating only the reinforced cue (simple). We additionally assessed the fit of a null model in which no learning happened. A Bayesian model comparison revealed that the inter-cue family of models outperformed the simple models (Figure S1) and that the inter-cue RW model provided the best fit to the data in most participants (Figure 2c). The distributions of the free parameters across participants show that for most participants, the expectation was a predictor of the SCR response (Figure 2d). A visual inspection of the model's predictions also supported a good fit to the data (Figures 2a and 2b).

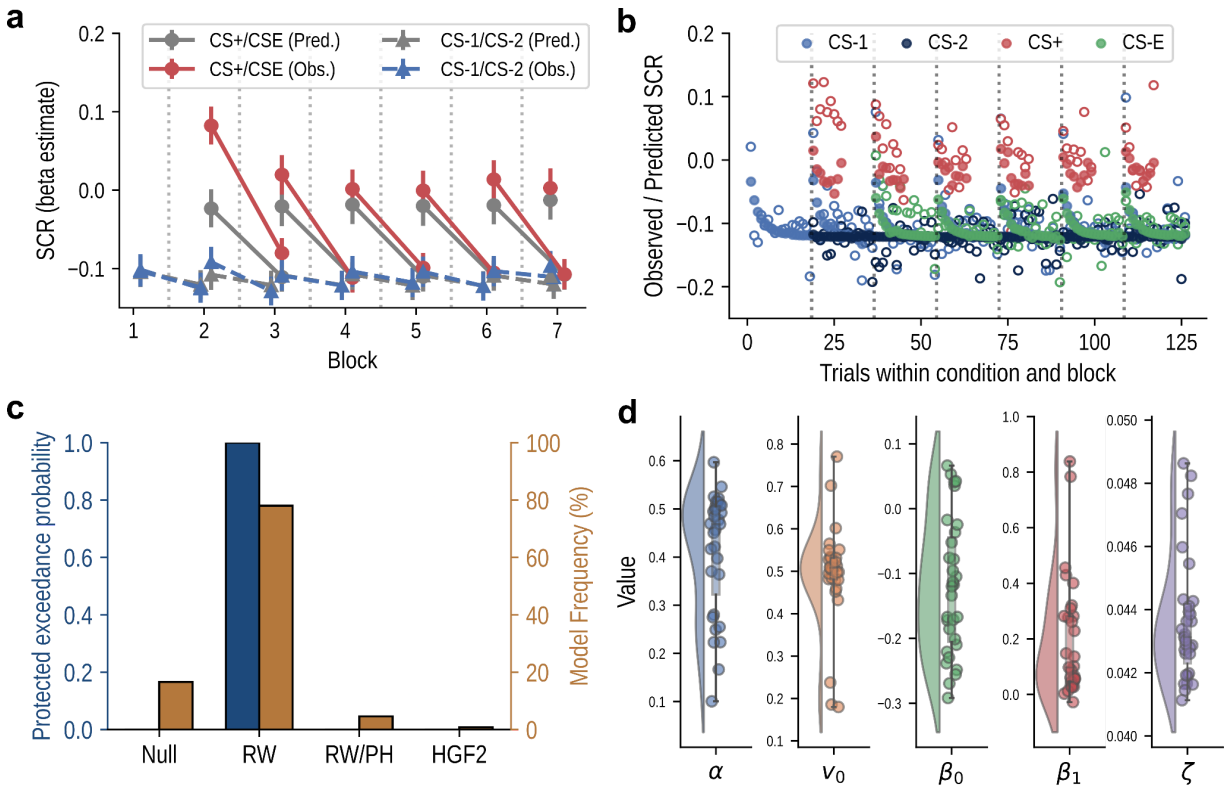

Figure 2. Skin conductance and computational model results. (a) Mean observed skin conductance response (Obs. colored) and mean predicted response (Pred. in gray) as a function of condition and experimental block. The lines between markers show the transition of one stimulus from one block to the next. Error bars show the standard error of the mean. **(b)** Observed (empty) and predicted (filled) SCR response for each trial. The dashed lines show the start of each experimental block. Note that reinforced trials were not predicted. **(c)** Results of the Bayesian model selection of the three inter-cue computational models showing the superiority of the Rescorla-Wagner model (RW) over a null model (no learning), as well as the combined RW/Pearce-Hall hybrid model (RW/PH) and the 2-level Hierarchical Gaussian Filter (HGF2) model. **(d)** Distributions of free parameters (see Methods) across participants for the winning RW model.

Prediction errors are associated with increased pain perception and physiological pain responses.

We tested the relationship between trial-wise PEs estimated using the RW model and pain responses. For cortical responses, we considered two commonly used EEG nociceptive responses, the amplitude of the N2-P2 component of the ERP and gamma band power (Figure 3a). We performed linear regressions between these two measures, the NFR amplitude, pain ratings and prediction errors at each trial within each participant and tested the significance of each relationship across participants using a two-tailed one-sample t-test on the slopes. We report results corrected for multiple comparisons using the Holm-Bonferroni procedure. This analysis revealed a significant relationship between the prediction error and all of the pain responses (Figure 3b and Figure 3c),

indicating that more surprising noxious stimuli led to increased physiological responses and were perceived as more intense.

We next assessed if PEs modulated pain responses through the spinal modulation of nociceptive activity as measured by the NFR. To this end, we performed multilevel mediations with the NFR as a mediator of the relationship between PEs and the other pain responses. The mediation models were implemented with the CanLab mediation toolbox (github.com/canlab/MediationToolbox; Wager et al., 2008, 2009) and we assessed the significance of each path using a bootstrap resampling procedure with 10 000 bootstrap samples. The NFR significantly mediated the relationship between PE and pain ratings and between PE and gamma power (Figure 3d). The mediation of the relationship between prediction error and N2-P2 amplitude by the NFR did not reach significance.

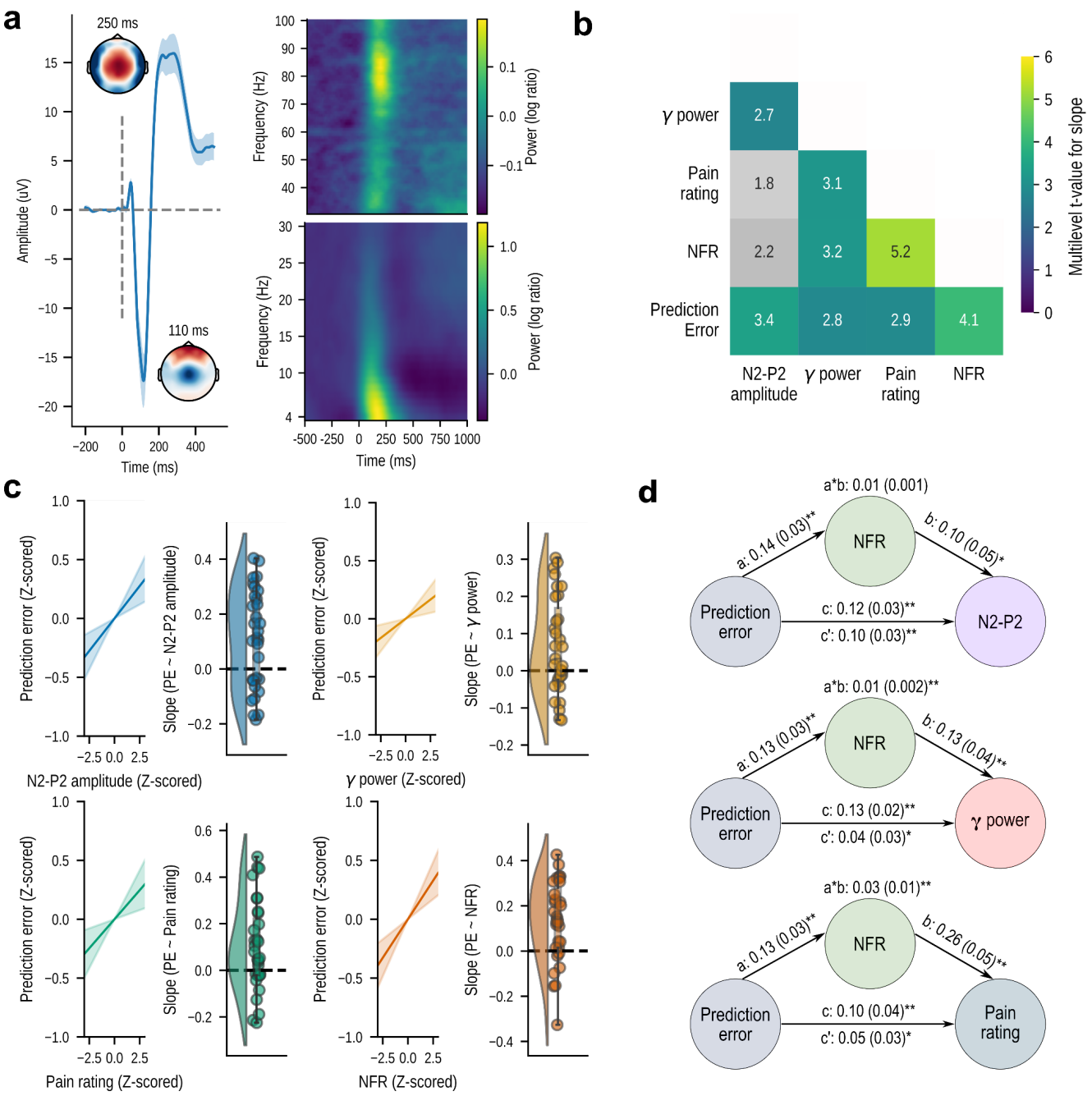

Figure 3. Pain responses and their relationship with prediction errors. (a) ERP response to the shock at CPz and topographic maps showing scalp distribution of the amplitude at each peak and TFR response to the shock at Cz showing the gamma band power. **(b)** Matrix showing the relationship between pain responses as the t-value for the second level test on the slopes of each participant. The colored squares show relationships surviving the Holm-Bonferroni corrected significance threshold and the gray squares show non-significant relationships. **(c)** Average and distribution of slopes across participants for the relationship of each pain response with prediction error. **(d)** Mediation of the relationships between prediction error and N2-P2 amplitude, gamma power and pain ratings by the NFR. *p < 0.05 **p < 0.005.

Prediction errors are associated with increased anticipatory cortical responses.

In order to identify the anticipatory signals giving rise to prediction errors and associated pain modulation, we evaluated the relationship between the anticipatory cortical responses to the cues and the trial-wise computational estimates of pain expectation, as well as pain ratings and NFR amplitudes for trials with electric shocks. To test the relationships between these variables and the trial-wise ERP amplitude and the time-frequency power, we used a mass univariate approach in which ordinary least square linear regressions were performed within each participant at each time point and location for ERP analyses or time point, location and frequency for time-frequency analyses. Beta values for each participant were then submitted to a two-tailed one-sample t-test comparing the group average beta value against 0 at each time point and location, and the results were corrected using cluster-based permutations with 5000 permutations, a cluster entering threshold of $p < .05$ two-tailed and a Bonferroni corrected cluster significance threshold of 0.05/3, two-tailed.

The amplitude of the late ERP response to pain predictive cues between 400 and 600 ms was closely related to the magnitude of the trial-wise computational estimate of pain expectation (Figure 4a). The mass univariate regression indicated that subjective pain expectation was significantly related to the ERP amplitude at parieto-occipital sites from 400 ms after the cue onset (Figure 4b). Pain expectations were also negatively related to anticipatory alpha and beta power. The results shown in Figures 4c and 4d reveal a significant negative relationship between pain expectation and the alpha and beta power at parieto-occipital sites and beta power at central sites. For both the ERP and TFR analyses, model-free analyses based on direct comparisons between the cue conditions revealed similar results (Supplementary Figure 2).

While a positive relationship between the late ERP amplitude at parieto-occipital sites was also observed for the pain ratings and NFR, the statistical tests of these relationships did not reach significance, and no clear relationship was observed between these two variables and time frequency power (Supplementary Figure 3).

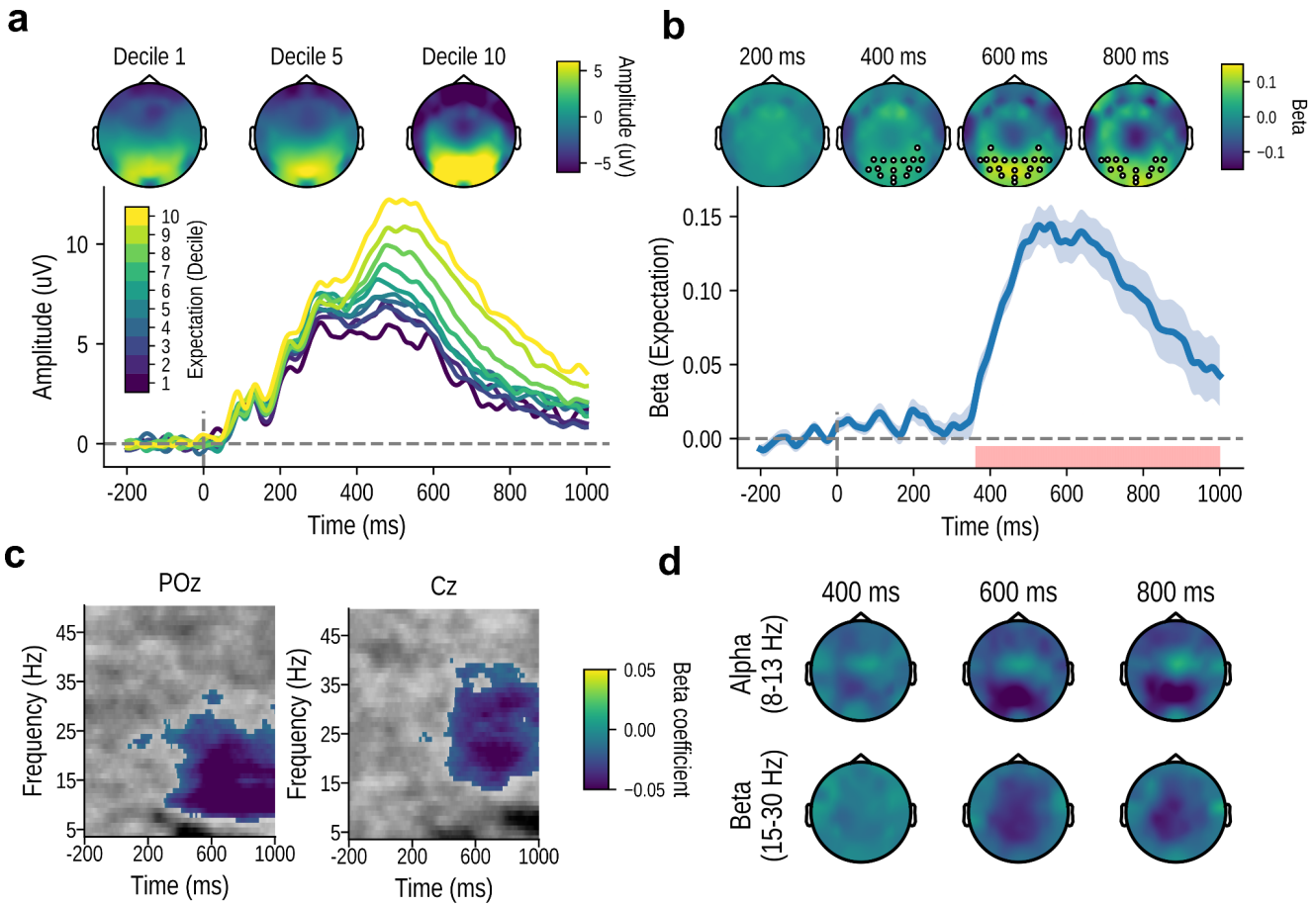

Figure 4. Results of the model-based analyses on the EEG response to the predictive cues. (a) Topographic map and ERP amplitude for various expectation levels at channel POz showing the increase in amplitude with the increase in pain expectation. **(b)** Beta estimates at POz (line plot) and at 200-800 ms (topographic plots) for the mass univariate regression of expectation on the ERP amplitude. The red lines and white circles show significant time points and locations ($p < 0.05$, cluster-based correction). **(c)** Beta coefficients for the mass univariate regression of pain expectation on TFR activity. The colored values show significant differences at $p < 0.05$, cluster-based correction. **(d)** Topographic maps illustrating the mean beta coefficients for the alpha and beta bands at different times.

Discussion

One of pain's primary functions is to teach us what may cause harm so that we can learn to avoid it in the future. This study sought to test the hypothesis that subjectively perceived pain is modulated by the informational value of nociceptive inputs. In support of that hypothesis, we found that subjective pain perception increases with the prediction error (PE) signals necessary to learn from surprising pain. Moreover, nociceptive flexion reflexes (NFRs) and EEG markers of cortical nociceptive processing (N2-P2 and gamma-band ERS) also increased with PEs, suggesting that prior expectations can influence the transmission of nociceptive signals from the spinal cord to the brain. Thus, nociceptive inputs to the brain appear to carry a PE signal that is essential for learning to predict the probability of future pain, suggesting that perceived pain is profoundly tied to its learning and adaptive function.

Our experimental paradigm was designed to produce frequent PEs by repeatedly introducing new conditioned stimuli during the task. Expectations about pain and PEs were estimated on a trial-by-trial basis by fitting different candidate learning models to the conditioned SCRs (Staib et al., 2015; Tzovara et al., 2018). This procedure indicated that a simple delta-rule Rescorla-Wagner model (Rescorla & Wagner, 1972) was the best fit for our data compared to other more complex models taking into account uncertainty (Mathys et al., 2014; Pearce & Hall, 1980). The reason why this simpler model provided a better fit could be because environmental volatility (Mathys et al., 2011) was kept relatively high and constant throughout the task due to the regular introduction of new cues.

Computational PE estimates predicted all dependent variables recorded in response to electric shocks, including pain ratings, NFR amplitude, N2–P2 amplitude, and gamma-band power. These findings are particularly interesting given that PE estimates were derived from the conditioned skin conductance responses to cues that were not followed by a shock. Modulation of NFR amplitude by PEs suggests that nociceptive signalling takes on a learning function as soon as nociceptive signals enter the central nervous system in the dorsal horn of the spinal

cord. This confirms the general notion that the main function of pain is to signify the need to adjust our behavior and not necessarily to accurately represent the intensity of the nociceptive stimulus (Craig, 2003; Klein, 2015).

The relationships between PEs and the N2-P2 amplitude and gamma-band power suggest that expectations can also affect the cortical response to nociceptive stimulation. Reduced cortical responses to pain when pain is expected likely reflect a downstream effect of reduced spinal nociception (Cormier et al., 2013; Goffaux et al., 2007; but see Martini et al., 2015). While this interpretation may hold for gamma-band power, as confirmed by the mediation analyses, it may not perfectly hold for N2-P2 amplitude, which did not significantly correlate with NFR amplitude or pain ratings. This aligns with previous studies suggesting that the N2-P2 component may not be specific to nociceptive input (Mouraux & Iannetti, 2009) but rather reflects general arousal and saliency. By contrast, previous research has suggested that gamma-band power may be a more specific measure of pain and nociception (Hu & Iannetti, 2019; Ploner & Gross, 2019), which may explain why we found stronger correlations between gamma-band power and NFRs and subjective pain ratings.

These findings correspond well with the notion that conditioned responses serve to prepare the organism for the upcoming homeostatic disturbance and therefore reduce the need to react to the painful stimulus itself (Steimer, 2002). This way, pain perception is reduced when pain is expected and amplified when unexpected. However, these findings conflict with prior studies showing that perceived pain is reduced when the expected probability of pain is low (Taylor et al., 2018, 2017). In this set of studies, cue-outcome contingencies remained stable for several trials and only reversed once in the middle of the experiment. In these studies, anticipatory SCRs were better fitted by a hybrid Pearce/Hall learning model with an associability term. Associability increases following surprising events to facilitate learning when the environment appears more uncertain. These studies found a positive relationship between associability and perceived pain and NFRs, and a negative relationship between PEs and pain and NFRs. By contrast, in the current experiment, associability was kept constantly high due to the frequent appearances of new cues, and we observed a positive relationship between pain and PEs.

One potential explanation for the apparently discrepant findings is that pain may be positively related to PEs when associability is high because participants actively try to predict pain, but are negatively related to PEs when associability is low.

Both model-based analyses using computationally derived estimates of pain expectations and model-free analyses using cue identity converged and showed that increased expectation of pain is linked to increased amplitude of the sustained late event-related potential response at parieto-occipital locations and increased alpha/beta decrease in power at occipital and centro-parietal sites starting around 400 ms after cue onset. These findings largely replicated previous studies on anticipatory responses to predictable aversive stimuli (Bacigalupo & Luck, 2018; Nickel et al., 2022; Pavlov & Kotchoubey, 2018; Sperl et al., 2020). The late positive potential is thought to reflect attentional allocation and motivational salience (Cuthbert et al., 2000; Hajcak et al., 2010) and might have reflected the threat value of the conditioned stimuli. By contrast, alpha/beta decrease in power is thought to reflect the priming of defensive motor responses (Babiloni, 2005; Babiloni et al., 2006). In the present experiment, alpha/beta power decreased with the proximity of potential pain, indicating that it might have reflected such preparatory processes.

The late positive potential and changes in oscillatory power anticipatory responses to the predictive cues were not significantly related to pain ratings or to the NFR amplitude. However, both anticipatory and pain responses were indirectly linked via their respective relationships with computational estimates of pain expectations and prediction errors. This pattern of results suggest that anticipatory responses are an indirect measure of expectations, and so expectations themselves (fitted to SCRs but constrained by the model) are a better predictor of pain than anticipatory activity. This is also supported by the observation that, as in previous work (Babiloni et al., 2006), the relationship between anticipatory responses and pain perception was positive. The lack of significance for these effects might be due to the relatively low number of reinforced trials available, limiting the examination of relationships with visually evoked responses at the single-trial level.

Results from this study should be replicated and extended in different contexts. One limitation of this study is the use of a repeated trial structure limiting the variability of the nature of the cue-pain associations. Future studies should assess the relationship between the informational value of nociceptive inputs and pain perception in an environment in which the probability of receiving pain after specific cues change over time, therefore creating more uncertainty (de Berker et al., 2016; Iglesias et al., 2013). Furthermore, in this study, participants passively experienced the pain stimulation and could not avoid them. It would be interesting to further assess the effect of the informational value of pain on pain perception when participants can perform choices based on the available information to avoid future pain.

In summary, we showed that computational estimates of learned pain expectations are associated with central anticipatory responses and pain perception. These results further strengthen the idea of a link between pain and learning and suggest that understanding the influence of learning mechanisms on pain could help us understand when and why pain perception is modulated in health and disease.

Materials and Methods

Participants

Thirty-five healthy participants with no history of neurological or pain disorders took part in the experiment. Four participants were excluded from all analyses due to unreliable SCR and technical issues or excessive noise in the EEG during recording. All analyses were thus performed on 31 participants (11 males, mean age: 23.39 years, SD=1.84). All participants provided written informed consent, and the experimental procedures were approved by the local ethics committee.

Stimuli

Visual Stimuli. Fourteen still frames showing neutral faces from different individuals (7 females) were selected from the Radboud Face Database (Langner et al., 2010) were grey-scaled and cropped to remove

non-facial features and served as the conditioned stimuli (CS). The stimuli-condition associations and presentation order were fully randomized.

Electrical Stimulations. The unconditioned stimulus (US) was presented simultaneously with the offset of the CS and consisted of a 30 ms transcutaneous electrical shock (10 x 1ms pulses at 333 Hz) delivered with a Grass s48 pulse simulator triggered by a computer running the E-Prime 2 software (Psychology Software Tools, Inc., Pittsburgh, USA). The electric shock was delivered to alcohol-cleaned skin over the right sural nerve with the electrodes placed behind the malleus of the right ankle. The shock intensity was calibrated to each participant's sensitivity using a staircase procedure, in which stimulation intensity was increased in small 0.5 mA increments until a reliable NFR was seen in the EMG. After eliciting three reflexes in a row, the ascending sequence changed to a descending sequence until observing a lack of reflex for three stimuli in a row. This procedure was repeated a total of three times. A logistic regression function was then fitted to predict the presence or absence of a reflex based on the intensity of the stimulation. The reflex threshold was determined by estimating the stimulus intensity associated with a 50% probability of eliciting a reflex. Stimulus intensity was set to be 135% of the threshold.

Procedure

Throughout the experiment, participants sat in an electrically shielded room. After the SCR and EMG recording electrodes were placed, the pain thresholding procedure was performed to determine the intensity of the electric shock that should be used for the task. Once the stimulation intensity was selected, the EEG cap was set up.

Participants were told they would see faces that may be followed by electric shocks and that the relationship between faces and shocks could change over time. They were instructed to look at the fixation cross and faces at all times. Finally, participants were asked to evaluate the pain induced by electrical stimulations using a visual analogue scale (VAS) with the labels "No pain" and "Worst pain imaginable" at each extremity (0 no pain

to 100 worst pain imaginable). The VAS was presented as a horizontal bar on a computer screen with the subject moving a cursor on the scale using a keyboard.

Participants then underwent the threat conditioning paradigm (see Figure 1a). The first block, represented by the gray column on the left side of Figure 1a, consisted in a habituation phase in which two faces are presented without any shocks. In the other six blocks one of the 4 presented faces is co-terminated with a shock for 50% of the trials and the other faces are never paired with the shock (CS-). Each presentation of the CS+ face was followed by a fixation cross of 2s and then the subjects were given a maximum of 10s to record their pain rating and to allow for the recording of the SCR. All trials started with an interstimulus interval (ISI) that was jittered between 5 to 7 seconds.

The presentation of the stimuli was divided into 7 blocks. Each face was presented 18 times in a single block for a total of 36 presentations of each face except the two last ones that were only presented for one block (18 times). Two new faces were presented each block with one of the new faces becoming the new CS+ face while the other remained CS-. CS+ faces in one block systematically became a CS-extinct (CS-E) face in the next block. The trials were presented in pseudo-random order, with the constraint that the first CS+ face of each block was always reinforced with a shock.

Physiological measures.

Electrodermal recordings and processing: Skin conductance responses (SCR) were recorded with a BIOPAC MP160 system combined with an EDA100C module using a pair of gelled electrodes positioned on the palm of the participant's right hand. The signal was amplified (5 µs/volt), bandpass filtered (1 -5 Hz) and sampled at 1000 Hz. SCRs were analyzed using the PsPM toolbox (Bach et al., 2010) within MATLAB (R2019a, The Mathworks Inc., Natick, MA). Skin conductance data were first preprocessed using PsPM's quality assurance script. PsPM's default values were used to remove and interpolate data points above or below 60 or 0.05 µS respectively or data points with a difference exceeding a slope of 10 µS/s. The data were then resampled to 10 Hz

and normalized before analysis. SCR to each stimulus was estimated using a general linear model (GLM) approach, by convolving a standard canonical SCR basis function with a time derivative to event onsets. We built a GLM for each trial which included the onset of the cue of the modeled trial as the regressor of interest and the onsets of the other cues, fixation crosses, shocks, rating screens and the onset of the recording as events of no interest. SCR amplitudes to the face cues were extracted using the reconstructed SCR (Bach et al., 2013) and used to fit the computational models. To confirm that conditioned cues elicited anticipatory SCR to a fear-conditioned cue and to assess the habituation of SCR responses across the experiment, we used a linear mixed-model with the factor Cue type (CS+, CS-E, CS-1, CS-2), Block (2-7) and their interaction as fixed effects and participants as random effects allowing for random intercepts. The contribution of each fixed effect was assessed by comparing the models with and without this factor using a likelihood ratio test.

Electromyographic (EMG) recordings and processing*:* Electromyographic activity of the biceps femoris was recorded through a pair of electrodes placed on the short head of the right biceps femoris, and a reference electrode placed on the tibial tuberosity. The skin regions were shaved, exfoliated and cleaned with alcohol before placing the electrodes. The EMG signal was amplified by a 1000 factor and sampled at 6250 Hz with a BIOPAC MP160 equipped with the EMG100C. The EMG signal was resampled to 1000 Hz and rectified using the root mean square (RMS) transform with a 15 ms time constant. Finally, the NFR amplitude was calculated as the RMS EMG area under the curve between 90 to 180 ms after the end of the electric shock.

EEG recordings and processing*:* EEG was recorded using 66 Ag-AgCl BioSemi Active Two electrode system (Biosemi Inc., Amsterdam, Netherlands) placed on the scalp according to the 10-10 international system and referenced to the mastoids. An electrooculogram (EOG) was recorded from 3 surface electrodes, two placed at the outer orbit of each eye horizontal to the pupil, and one placed below the left eye vertical to the pupil. Signals were amplified and digitized at a sampling rate of 1024 or 2024 Hz.

All EEG analyses were performed using MNE-python (Gramfort et al., 2013). The data were first resampled to 1024Hz if acquired at a higher rate and high-pass filtered at 0.1 Hz using a zero-phase non-causal finite impulse response (FIR) filter. Bad channels were identified via visual inspection and removed from the data for independent component analyses (mean number of bad channels: 1.68, SD=1.25, range=0-5). An independent component analysis (ICA) was performed using the *fastica* algorithm. Before ICA, the data were additionally bandpass filtered between 1 and 100 Hz, segmented -0.5 to 1 s around cues onsets and segments with a value exceeding 500 uV were dropped. The ICA cleaning procedure was performed separately for EEG responses to visual cues and electrical shocks. For visual cues, artifactual components associated with eye blinks or movements were removed from the data (mean number of components removed: 2.25, SD=1.0, range:1-4). For electrical shocks, we followed the recommendations of Liebisch et al., 2021 and removed all components with apparent muscle spikes (mean number of components removed: 12.38, SD=3.79, range: 4-22). After ICA, the data were re-referenced to the average reference and removed channels were interpolated using neighbouring channels.

For ERP analyses, the EEG data were additionally low-pass filtered at 30 Hz before event-related potential (ERP) analyses. The data was segmented -0.2 to 1 s around the onset of the face cue or the shock stimulation and baseline-corrected by subtracting the mean pre-stimulus value. Segments with values exceeding +/- 500 µV were excluded from further analyses, which led to the removal of an average of 2.62 % of trials (SD=3.74, range:0-16.67%) with a final average number of trials of 141.06 (SD=3.97, range:125-144) trials for the CS-1 condition, 123.12 (SD=4.92, range: 102-126) trials for CS-2, 105.25 (SD=4.32, range: 90-108) trials for CS+, 88.12 (SD=3.91, range: 70-90) trials for CS-E and 50.74 (SD=6.64, range: 23-54) trials for shocks. The N2-P2 evoked potential in response to the shock was measured as the difference between the peak amplitude between 200 and 500 ms and the preceding negative peak between 50 to 200 ms after the onset of the shock.

For TFR analyses, the continuous EEG data segmented -2 to 2 s around the onset of the face cue or the shocks for the time-frequency analysis. To avoid capturing the response to the electrical shocks into the time-frequency response to the cue, only non-reinforced trials were analyzed for analyses of the time-frequency response to the visual cue unless otherwise specified. All trials rejected from the ERP analyses were also removed from the time-frequency analyses. The time-frequency representation (TFR) of each trial was obtained using a Morlet wavelet transform with a frequency range of 4 to 100 Hz and a resolution of 1 Hz and cycle sizes of $0.5*f$. The resulting time-frequency representations (TFR) were downsampled in time to 256 Hz, baseline corrected by taking the log of the ratio of each value and the -0.5 to -0.2 s pre-stimulus period and cropped to -0.2 to 1 s for subsequent statistical analyses. Gamma band power in response to the shock was measured as the mean power between 120 to 250 ms and 60 to 85 Hz after the onset of the shock.

Computational Modeling

We considered three learning models to explain the trial-wise anticipatory SCR responses: the Rescorla-Wagner model (RW), the Rescorla-Wagner/Pierce-Hall hybrid model (RW/PH) (Rescorla & Wagner, 1972; Pearce-Hall 1980) and the Hierarchical Gaussian Filter (HGF; Mathys et al., 2011; Mathys et al., 2014). Two versions of each model were run. In the first version, the model was fitted for each cue without considering the influence of other cues (cue-specific). In a second version, the information about other seen cues is updated simultaneously when a cue is reinforced (inter-cue). Bayesian model comparison indicated that the inter-cue family of models showed an overall better fit to our data (exceedance probability of the intercue family: 0.90, model frequency: 61%) and only these models were further considered in addition to a null model in which no learning occurred. All models were fitted to participants' individual trial-wise SCR using the TAPAS toolbox (https://github.com/translationalneuromodeling/tapas). Where priors were required for the HGF models, we selected them by inverting the perceptual model in isolation for each participant under suitably uninformative priors and used the group average of each parameter as prior. Trials that were reinforced or that were more than three

deviations away from the participant's mean SCR were ignored in the model fitting. The Log-model evidence (LME) was used to assess model fit using a random-effect Bayesian model selection implemented in the Variational Bayesian Analysis toolbox (VBA; https://mbb-team.github.io/VBA-toolbox; Daunizeau et al., 2014).

Null model

Perceptual model. We included a null model to ensure that our learning models would fit the data better than a model in which no learning occurred. The null model considered that participants could perfectly predict the occurence of the shock:

$$V_t = \begin{cases} 1 \text{ if } \lambda = 1 \\ 0 \text{ if } \lambda = 0 \end{cases} \quad (1)$$

Where V is the expected probability and λ is the reinforcement value.

Response model. The response model for the null model considered that the SCR was linearly related to the perfect prediction of the shock:

$$(2)\ SCR = B_0 + B_1 * V$$

Rescorla-Wagner model.

Perceptual Model. The RW depends on prediction errors to direct associative changes, such that larger errors between the actual and expected value will drive larger changes in associative strength (Resocorla & Wagner, 1972). The basic RW model is defined by equations 1 below where *V* is the expected shock probability which is updated every trial (t) according to the learning rate parameter α, the difference between the actual outcome and expected outcome (δ), λ the reinforcement value (shock = 1, no shock = 0), and *V* the expected probability.

$$(3)\ V_{t+1} = V_i + \alpha * \delta_t$$

$$(4)\ \delta_t = \lambda_t - V_i$$

At the first presentation of each cue the expected probability corresponds to the fitted initial value, $V_i = V_0$. After each update, the updated expected value of the cue i is stored for future retrieval:

$$(5)\ V_i = V_{t+1}$$

And cue i is added to the set of seen cues:

$$(6)\ i \in Seen$$

When a shock is delivered, each cue in the ensemble of all previously seen cues but not presented at trial t is updated using equations 1 and 2 with $\lambda = 0$ and the corresponding updated expected value is stored for each cue for future retrieval.

Response model. The RW response model considered that the SCR amplitude at each trial was linearly related to the expected value with the addition of Gaussian noise (ζ).

$$(7)\ SCR = B_0 + B_1 * V + \zeta$$

Rescorla-Wagner/Pearce-Hall Hybrid

Perceptual model. In the RW/PH model, the learning rate is influenced by the amount of attention devoted to the cue after a surprising outcome represented by an associability term (Pearce-Hall 1980). If there is a large error between the actual and expected outcome (e.g. a surprising event), this will result in an increased amount of attention being given to the relevant cues in order to learn associations; in contrast, small or no errors will hamper learning (Pearce-Hall 1980). The hybrid model incorporates the PH into the RW model by updating reinforcement expectation by allowing for modulation of the learning rate (α) based on the degree of surprise regarding the event.

$$(8)\ V_{t+1} = V_i + a_i * \alpha * \delta_t$$

$$(9)\ \delta_t = \lambda_t - V_i$$

$$(10)\ a_{t+1} = \gamma * |\delta_t| + (1-\gamma) * a_i$$

Where *t* is the trial number, *i* is the identity of the presented cue at trial t, α the learning rate, δ the prediction error, λ the reinforcement value, *V* the expected probability, a the associability and γ is a discount factor that determines how much a is influenced by events on the immediately preceding trials. At the first presentation of each cue, the expected probability and the associability correspond to the fitted initial value; $V_i = V_0$, $a_i = a_0$. After each update, the updated expected value and associability of cue i are stored for future retrieval:

$$(11)\ V_i = V_{t+1}$$

$$(12)\ a_i = a_{t+1}$$

and cue i is added to the ensemble of seen cues (equation 3). When a shock is delivered, the expected value and associability of each previously seen cue but not presented at trial *t* is updated using equations 7, 8 and 9 with $\lambda = 0$ and the corresponding updated expected value and associability are stored for each cue.

Response model. Based on previous reports indicating that the SCR response is best characterized as a mixture of expectation and uncertainty, the RW/PH response model considered that SCR amplitude at each trial was linearly related to the expected value and associability with the addition of Gaussian noise.

$$(12)\ SCR = B_0 + B_1 * V + B_2 * a + \zeta$$

Hierarchical Gaussian Filter

Perceptual Model. The HGF consists of a perceptual and response model of an ideal Bayesian observer who is receiving inputs from the environment and has behavioural outputs (or responses, Mathys et al., 2011). We used the standard two-level HGF for binary responses. As in the RW and RW/PH models described above, previously seen cues were updated with a negative prediction error when another cue was reinforced. Since the HGF was not found to outperform the RW model in the current experiment, for the sake of brevity, we refer the

reader to previous descriptions of this model for the updated equations (Mathys et al., 2011, 2014) and to the open code for details on the current implementation.

Response models Similarly to the RW/PH model, the HGF response model included both the participants' expectations and uncertainty at the first level:

$$SCR = B_0 + B_1 * \hat{\mu}_1 + B_2 * \hat{\sigma}_1 + \zeta \tag{13}$$

References

Babiloni, C. (20050418). Expectancy of Pain Is Influenced by Motor Preparation: A High-Resolution EEG Study of Cortical Alpha Rhythms. *Behavioral Neuroscience*, *119*(2), 503. https://doi.org/10.1037/0735-7044.119.2.503

Babiloni, C., Brancucci, A., Percio, C. D., Capotosto, P., Arendt-Nielsen, L., Chen, A. C. N., & Rossini, P. M. (2006). Anticipatory Electroencephalography Alpha Rhythm Predicts Subjective Perception of Pain Intensity. *The Journal of Pain*, *7*(10), 709–717. https://doi.org/10.1016/j.jpain.2006.03.005

Bach, D. R., Flandin, G., Friston, K. J., & Dolan, R. J. (2010). Modelling event-related skin conductance responses. *International Journal of Psychophysiology*, *75*(3), 349–356. https://doi.org/10.1016/j.ijpsycho.2010.01.005

Bach, D. R., Friston, K. J., & Dolan, R. J. (2013). An improved algorithm for model-based analysis of evoked skin conductance responses. *Biological Psychology*, *94*(3), 490–497. https://doi.org/10.1016/j.biopsycho.2013.09.010

Bacigalupo, F., & Luck, S. J. (2018). Event-related potential components as measures of aversive conditioning in humans. *Psychophysiology*, *55*(4). https://doi.org/10.1111/psyp.13015

(Bud) Craig, A. D. (2003). A new view of pain as a homeostatic emotion. *Trends in Neurosciences*, *26*(6), 303–307. https://doi.org/10.1016/S0166-2236(03)00123-1

Cormier, S., Piché, M., & Rainville, P. (2013). Expectations Modulate Heterotopic Noxious Counter-Stimulation Analgesia. *The Journal of Pain*, *14*(2), 114–125. https://doi.org/10.1016/j.jpain.2012.10.006

Cuthbert, B. N., Schupp, H. T., Bradley, M. M., Birbaumer, N., & Lang, P. J. (2000). Brain potentials in affective picture processing: Covariation with autonomic arousal and affective report. *Biological Psychology*, *52*(2), 95–111. https://doi.org/10.1016/S0301-0511(99)00044-7

Daunizeau, J., Adam, V., & Rigoux, L. (2014). VBA: A Probabilistic Treatment of Nonlinear Models for Neurobiological and Behavioural Data. *PLOS Computational Biology*, *10*(1), e1003441. https://doi.org/10.1371/journal.pcbi.1003441

de Berker, A. O., Rutledge, R. B., Mathys, C., Marshall, L., Cross, G. F., Dolan, R. J., & Bestmann, S. (2016). Computations of uncertainty mediate acute stress responses in humans. *Nature Communications*, *7*(1). https://doi.org/10.1038/ncomms10996

Garcia-Larrea, L., Frot, M., & Valeriani, M. (2003). Brain generators of laser-evoked potentials: From dipoles to functional significance. *Neurophysiologie Clinique/Clinical Neurophysiology*, *33*(6), 279–292. https://doi.org/10.1016/j.neucli.2003.10.008

Goffaux, P., Redmond, W. J., Rainville, P., & Marchand, S. (2007). Descending analgesia – When the spine echoes what the brain expects. *PAIN*, *130*(1), 137–143. https://doi.org/10.1016/j.pain.2006.11.011

Gramfort, A., Luessi, M., Larson, E., Engemann, D. A., Strohmeier, D., Brodbeck, C., Goj, R., Jas, M., Brooks, T., Parkkonen, L., & Hämäläinen, M. (2013). MEG and EEG data analysis with MNE-Python. *Frontiers in Neuroscience*, *7*. https://doi.org/10.3389/fnins.2013.00267

Hajcak, G., MacNamara, A., & Olvet, D. M. (2010). Event-Related Potentials, Emotion, and Emotion Regulation: An Integrative Review. *Developmental Neuropsychology*, *35*(2), 129–155. https://doi.org/10.1080/87565640903526504

Henrich, M. C., Frahm, K. S., Coghill, R. C., & Andersen, O. K. (2022). Spinal Nociception is Facilitated during Cognitive Distraction. *Neuroscience*, *491*, 134–145. https://doi.org/10.1016/j.neuroscience.2022.03.038

Herry, C., & Johansen, J. P. (2014). Encoding of fear learning and memory in distributed neuronal circuits. *Nature Neuroscience*, *17*(12), 1644–1654. https://doi.org/10.1038/nn.3869

Hu, L., & Iannetti, G. D. (2019). Neural indicators of perceptual variability of pain across species. *Proceedings of the National Academy of Sciences*, *116*(5), 1782–1791. https://doi.org/10.1073/pnas.1812499116

Iglesias, S., Mathys, C., Brodersen, K. H., Kasper, L., Piccirelli, M., den Ouden, H. E. M., & Stephan, K. E. (2013).

Hierarchical Prediction Errors in Midbrain and Basal Forebrain during Sensory Learning. *Neuron*, *80*(2), 519–530. https://doi.org/10.1016/j.neuron.2013.09.009

Jepma, M., Roy, M., Ramlakhan, K., van Velzen, M., & Dahan, A. (2022). Different brain systems support learning from received and avoided pain during human pain-avoidance learning. *ELife*, *11*, e74149. https://doi.org/10.7554/eLife.74149

Klein, C. (2015). *What the body commands: The imperative theory of pain*. MIT Press.

Langner, O., Dotsch, R., Bijlstra, G., Wigboldus, D. H. J., Hawk, S. T., & van Knippenberg, A. (2010). Presentation and validation of the Radboud Faces Database. *Cognition and Emotion*, *24*(8), 1377–1388. https://doi.org/10.1080/02699930903485076

Liebisch, A. P., Eggert, T., Shindy, A., Valentini, E., Irving, S., Stankewitz, A., & Schulz, E. (2021). A novel tool for the removal of muscle artefacts from EEG: Improving data quality in the gamma frequency range. *Journal of Neuroscience Methods*, *358*, 109217. https://doi.org/10.1016/j.jneumeth.2021.109217

Linde, L. D., Ortiz, O., Choles, C. M., & Kramer, J. L. K. (2023). Pain-related gamma band activity is dependent on the features of nociceptive stimuli: A comparison of laser and contact heat. *Journal of Neurophysiology*, *129*(1), 262–270. https://doi.org/10.1152/jn.00357.2022

Martini, M., Lee, M. C. H., Valentini, E., & Iannetti, G. D. (2015). Intracortical modulation, and not spinal inhibition, mediates placebo analgesia. *European Journal of Neuroscience*, *41*(4), 498–504. https://doi.org/10.1111/ejn.12807

Mathys, C. D., Lomakina, E. I., Daunizeau, J., Iglesias, S., Brodersen, K. H., Friston, K. J., & Stephan, K. E. (2014). Uncertainty in perception and the Hierarchical Gaussian Filter. *Frontiers in Human Neuroscience*, *8*. https://doi.org/10.3389/fnhum.2014.00825

Mathys, C., Daunizeau, J., Friston, K., & Stephan, K. (2011). A Bayesian Foundation for Individual Learning Under Uncertainty. *Frontiers in Human Neuroscience*, *5*. https://www.frontiersin.org/articles/10.3389/fnhum.2011.00039

McNally, G. P., Johansen, J. P., & Blair, H. T. (2011). Placing prediction into the fear circuit. *Trends in Neurosciences*, *34*(6), 283–292. https://doi.org/10.1016/j.tins.2011.03.005

Mouraux, A., & Iannetti, G. D. (2009). Nociceptive laser-evoked brain potentials do not reflect nociceptive-specific neural activity. *Journal of Neurophysiology*, *101*(6), 3258–3269. WorldCat.org. https://doi.org/10.1152/jn.91181.2008

Nickel, M. M., Tiemann, L., Hohn, V. D., May, E. S., Ávila, C. G., Eippert, F., & Ploner, M. (2022). Temporal–spectral signaling of sensory information and expectations in the cerebral processing of pain. *Proceedings of the National Academy of Sciences*, *119*(1). https://doi.org/10.1073/pnas.2116616119

Pavlov, Y. G., & Kotchoubey, B. (2018). *Aversive conditioning in oddball paradigm modulates multisensory integration, attention and emotional processing* [Preprint]. Neuroscience. https://doi.org/10.1101/286492

Pearce, J. M., & Hall, G. (1980). A model for Pavlovian learning: Variations in the effectiveness of conditioned but not of unconditioned stimuli. *Psychological Review*, *87*(6), 532.

Ploner, M., & Gross, J. (2019). Gamma Oscillations Shape Pain in Animals and Humans. *Trends in Cognitive Sciences*, *23*(6), 450–451. https://doi.org/10.1016/j.tics.2019.04.001

Price, D. D. (2000). Psychological and Neural Mechanisms of the Affective Dimension of Pain. *Science*, *288*(5472), 1769–1772. https://doi.org/10.1126/science.288.5472.1769

Rescorla, R. A., & Wagner, A. (1972). A theory of Pavlovian conditioning: Variations in the effectiveness of reinforcement and nonreinforcement. *Current Research and Theory*, 64–99.

Roy, M., Shohamy, D., Daw, N., Jepma, M., Wimmer, G. E., & Wager, T. D. (2014). Representation of aversive prediction errors in the human periaqueductal gray. *Nature Neuroscience*, *17*(11), 1607–1612. https://doi.org/10.1038/nn.3832

Rütgen, M., Seidel, E.-M., Riečanský, I., & Lamm, C. (2015). Reduction of Empathy for Pain by Placebo Analgesia Suggests Functional Equivalence of Empathy and First-Hand Emotion Experience. *Journal of*

Neuroscience, *35*(23), 8938–8947. https://doi.org/10.1523/JNEUROSCI.3936-14.2015

Seymour, B. (2019). Pain: A Precision Signal for Reinforcement Learning and Control. *Neuron*, *101*(6), 1029–1041. https://doi.org/10.1016/j.neuron.2019.01.055

Sperl, M. F. J., Wroblewski, A., Mueller, M., Straube, B., & Mueller, E. M. (2020). Learning Dynamics of Electrophysiological Brain Signals During Human Fear Conditioning. *NeuroImage*, 117569. https://doi.org/10.1016/j.neuroimage.2020.117569

Staib, M., Castegnetti, G., & Bach, D. R. (2015). Optimising a model-based approach to inferring fear learning from skin conductance responses. *Journal of Neuroscience Methods*, *255*, 131–138. https://doi.org/10.1016/j.jneumeth.2015.08.009

Steimer, T. (2002). The biology of fear- and anxiety-related behaviors. *Dialogues in Clinical Neuroscience*, *4*(3), 231–249.

Strube, A., Rose, M., Fazeli, S., & Büchel, C. (2021, February 17). *The temporal and spectral characteristics of expectations and prediction errors in pain and thermoception*. ELife; eLife Sciences Publications Limited. https://doi.org/10.7554/eLife.62809

Sutton, R. S., & Barto, A. G. (2018). *Reinforcement learning: An introduction* (Second edition). The MIT Press.

Taylor, Roy, M., Chang, L., Gill, L.-N., Mueller, C., & Rainville, P. (2018). Reduced Fear-Conditioned Pain Modulation in Experienced Meditators: A Preliminary Study. *Psychosomatic Medicine*, 1. https://doi.org/10.1097/PSY.0000000000000634

Taylor, V. A., Chang, L., Rainville, P., & Roy, M. (2017). Learned expectations and uncertainty facilitate pain during classical conditioning: *PAIN*, *158*(8), 1528–1537. https://doi.org/10.1097/j.pain.0000000000000948

Tzovara, A., Korn, C. W., & Bach, D. R. (2018). Human Pavlovian fear conditioning conforms to probabilistic learning. *PLOS Computational Biology*, *14*(8), e1006243. https://doi.org/10.1371/journal.pcbi.1006243

Wager, T. D., Davidson, M. L., Hughes, B. L., Lindquist, M. A., & Ochsner, K. N. (2008). Prefrontal-subcortical pathways mediating successful emotion regulation. *Neuron*, *59*(6), 1037–1050. https://doi.org/10.1016/j.neuron.2008.09.006

Wager, T. D., Waugh, C. E., Lindquist, M., Noll, D. C., Fredrickson, B. L., & Taylor, S. F. (2009). Brain mediators of cardiovascular responses to social threat: Part I: Reciprocal dorsal and ventral sub-regions of the medial prefrontal cortex and heart-rate reactivity. *NeuroImage*, *47*(3), 821–835. https://doi.org/10.1016/j.neuroimage.2009.05.043